NOISE REDUCTION OF A LARGE AXIAL FLOW FAN FOR CSP AIR-COOLED CONDENSERS

Gino ANGELINI[1], David VOLPONI[1], Mike B. WILKINSON[2], Sybrand J. van der SPUY[2], Tommaso BONANNI[1], Lorenzo TIEGHI[1], Giovanni DELIBRA[1], Alessandro CORSINI[1] and Theodor W. von BACKSTRÖM[2]

[1] *Sapienza University of Rome, Dipartimento di Ingegneria Meccanica e Aerpspaziale, Via Eudossiana 18, 00184 Roma, Italy*

[2] *Stellenbosch University, Department of Mechanical Engineering, Stellenbosch, Private Bag X1, 7602, South Africa*

SUMMARY

In this paper we focus on two different strategies to reduce the noise of the M-Fan, designed and manufactured to operate in an air-cooled condenser for CSP power plants. The first round of optimization was carried out coupling an axis-symmetric flow solver (AxLab) with an optimization software based on brute force optimization. The procedure aimed at optimizing the chord and pitch distribution of the M-Fan to reduce trailing edge noise and increase the fan efficiency. The second approach was based on challenging the paradigm of design vortex distribution of work along the blade span. In particular a power law distribution was selected, aiming at unloading the tip and control the tip leakage vortex.

INTRODUCTION

In regions with limited availability of fresh water, air-cooled condensers (ACCs) are used in thermal power plants with steam cycles. In ACCs, axial flow fans are used to force fresh air through heat exchangers with bundle of tubes. These fans are characterized by operations at very high flow rates (> 250 m^3/s), large diameters (> 7 m), limited rotational speed (100-200 rpm) and very low pressure rise capability (< 250 Pa). Fans in ACCs have two major requests from the market: decrease power consumption and noise emissions. This is related to the fact that ACCs work with huge arrays of fans (300-600 units) and therefore impact abruptly on the overall system efficiency of the power plant. At the same time such arrays of fans are really noisy and, even if usually installed in remote areas, lowering noise is still an issue. Noise reduction strategies must take into account the fact that these fans have a rotor-only arrangement and therefore it is not possible to

work on the coupling with an outlet guided vane and, given the large diameter and complex installation issues, it is practically impossible to have a strict control on the tip-gap or even in the perfect shape of the fan casing. It is, however, possible to apply flow-control strategies to reduce noise related to tip-leakage-vortex, such as tip-endplates [1]-[3], or to control the wake such as leading edge bumps [4]. Another source of noise, typically related to trailing edge bluntness can be controlled by optimization of the twist and chord distributions of the blade [5]. To this aim here we present an optimization process based on an axial-symmetric Python code (AxLab) that applies the model described in [5] to compute trailing edge noise. The optimization process relies on brute force algorithm that explores all the possible combinations of pitch and chord spanwise distribution and generates a population of 200.000 individuals to be tested with AxLab to verify their air performance and trailing edge noise with Fukano's model [5]. Finally CFD computations are used to verify the design point performance of the individual chosen among those with better performance. Then noise reduction was verified by post-processing the flow field and re-applying the model in [5] to numerical results.

OPTIMIZATION PROCESS

Numerical design optimization was used to minimize the trailing edge noise of a single stage axial fan. The blade of the rotor was divided into 11 control sections; on these two geometric variables were varied (chord and pitch) to provide a wide database of optimized individuals, that can be used to search for solutions that can satisfy different geometrical constraints. Imposed constraints assured the same total pressure rise delivered from the baseline fan. A blade element model was used to evaluate the aerodynamic performance of the fan and trailing edge noise. One potential design was selected from the set of simulations and the comparison with the baseline blade showed that it is possible to obtain an individual that both can reduce noise generation and increase the total to total efficiency.

Methodology

A relevant noise source in the baseline fan is produced by the trailing edge, as with these large fans trailing edge bluntness in unavoidable to respect mechanical constraints. Trailing edge noise is caused by the vorticity shed from the trailing edge which produces local lift fluctuations. In the present study, a model for the trailing edge noise was combined with an aerodynamical model for rotor-only fans. For a given rotor geometry and fan operating conditions, the analysis tool provided the trailing edge noise and flow characteristics (e.g., velocity triangles, fan efficiency and pressure rise). Numerical model used for the generation of the database is implemented in AxLab, a tool for performance analysis of ducted axial fans. This software is based on a blade element axisymmetric principle. The rotor blade is divided into 11 streamlines. For each of these streamlines relations for velocity triangles and pressure are derived from incompressible conservation laws for mass, tangential momentum and energy. The complexity of 3D flow is partially reproduced by the juxtaposition of the flow conditions on the meridional plane and the circumferential plane. The analysis model for the noise emission is based on the model developed by Fukano et al [5].

Description of the baseline blade (M-Fan)

The baseline blade, here labelled as M-Fan, is a single stage axial fan for cooling of CSP plants. The duty point of baseline blade presents an uncommon combination of dimensionless global duty parameters: a load coefficient of 0.11, a flow coefficient of 0.23 and a static efficiency > 0.6. Hub to tip ratio is equal to 0.3. Airfoil thickness distribution used for each section is an optimized version

of NASA LS 417 distributed on a circular arc camber line. Geometry of the baseline blade is represented inside AxLab software [6] by means of eleven radial blade sections. In Figure 1 fan performance charts predicted by Axlab are shown in normalized variables.

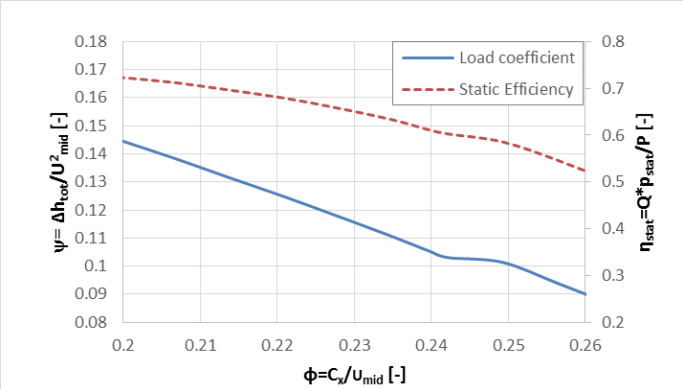

Figure 1 - static efficiency η_{stat} and load coefficient ψ vs flow coefficient φ

Pitch and chord optimization

Optimization process takes into account both variation in pitch angle and blade chord of each section of the blade. To identify the variation of pitch and chord distributions, the following methodology was selected:

- along the blade span are identified a number of reference sections N_{ref} ;
- on each of those sections, pitch and chord distributions are varied assuming a number of possible discrete values, Figure 2.

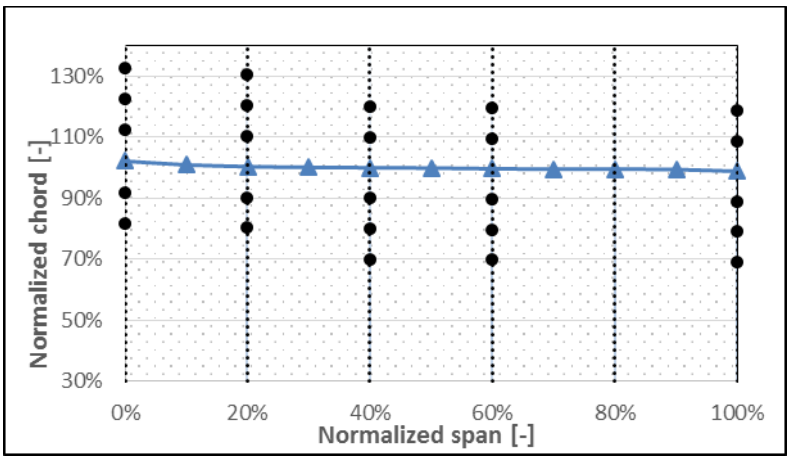

Figure 2 - Range of chord length variation with evidenced reference sections Nref and nodes K

During pitch optimization were selected 6 reference sections and for each of those section 7 nodes. Nodes were selected considering a pitch variation of the M-Fan of +/- 30 %, +/- 20 %, +/- 10 % and 0 %. Instead for the chord length optimization were selected 5 reference sections and for each of those 6 nodes considering a chord variation of the configuration of the M-Fan of + 30 %, +/- 20 %, +/- 10 % and 0 % for the first two reference sections while for the rest - 30%, +/- 20 %, +/- 10% and 0% (see Figure 2). To avoid excessive distorted or unrealistic geometries we decided to restrict possible geometries to those respecting the following criteria:

1. Decreasing pitch: $\xi\,(R_i) < \xi\,(R_{i+1} > R_A)$;
2. Limited pitch distortion: $\xi\,(R_i) - \xi\,(R_{i+1}) < 8°$;
3. Limited chord distortion: $l_c\,(R_i) - l_c\,(R_{i+1}) \leq 0.1\ m$;
4. Weight limit: $\text{weight}_{\text{Baseline blade}} < \text{weight}_{\text{Individual}}$.

where R_i is the radius of reference i-section and R_{i+1} is the radius of the following section. Application of constraints 1-4 reduces the number of individuals from ~ 6×10^{11} to 206 275 reducing the computational cost to 2/1000. Blade weight was simply evaluated numerically integrating the chord length across the blade span, considering a linear thickness distribution from 13 % to 9 %. Each simulation was run with AxLab on a Linux server using 40 processors and the total computational time was of about 7 days. The software evaluates every geometry. If the total pressure rise provided results different from the imposed value, hub pitch (ξ_{hub}) of the blade is modified to obtain the target value with an error of 0.1 % on total pressure rise.

All tested configuration were stored into a database: each element is identified by values of gain in terms of total efficiency $\Delta\eta_{tot}$ and reduction in sound pressure level ΔSPL. In Figure 3 results from the database with all tested configuration are presented, with the M-Fan as datum geometry and L3C2 individual as the chosen optimized rotor highlighted with specific symbols.

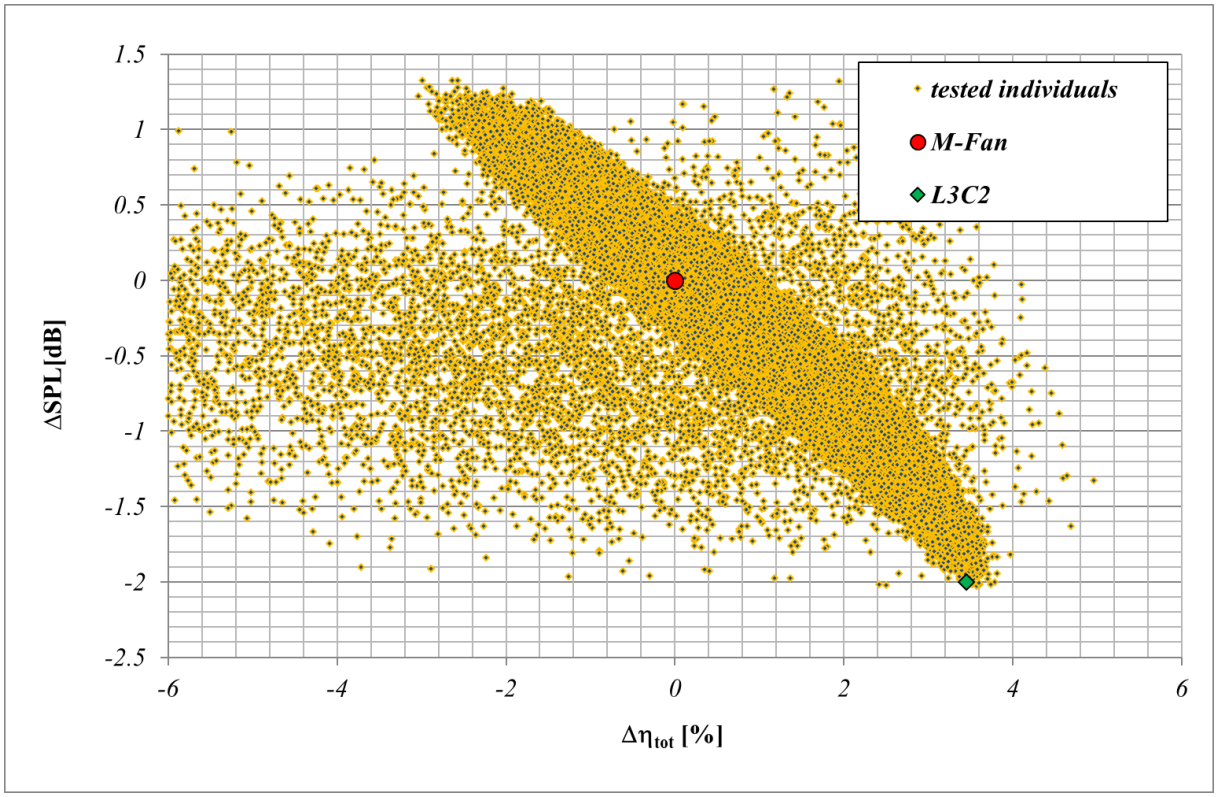

Figure 3 - Database of simulations performed during pitch and chord optimization

Results demonstrate that a notable noise reduction and efficiency increase can be obtained. Even if it is difficult to clearly identify a selection of optimal solutions (e.g. a Pareto Front), one element, here identified with L3C2, was selected from all the data following the main goal of increasing η_{tot} and to decrease as much as possible SPL. Table 1 summarizes the performance of this candidate.

Table 1- Selected individual features in terms of static efficiency and noise emission

Individual name	η_{stat} [%]	*SPL*[dB]	$\Delta\eta_{stat}$[%]	ΔSPL[dB]	ξ_{hub} [deg]
L3C2	64.003	95.630	2.783	-1.9745	-2.767

The first result of this optimization process is that the L3C2 fan reduced the blade weight of 10 % and incremented the fan static efficiency more than 2 %. Also results on blade noise emission seems to be promising. Figure 4 shows a comparison of the chord and pitch distributions of the L3C2 with respect to those of the M-Fan.

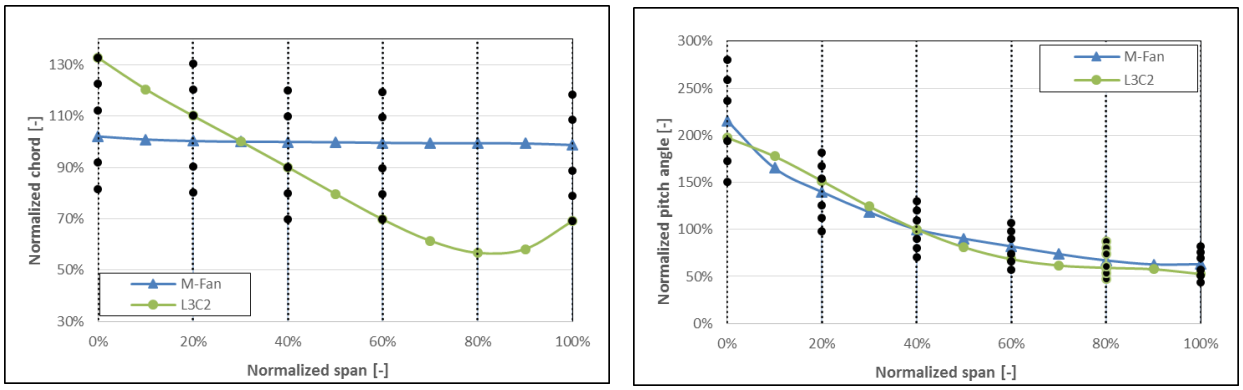

Figure 4 - (a) chord variation of Optimized blade; (b) pitch variation of Optimized blade

CFD ANALYSIS

Solvers and numerical schemes

Computations were carried out with the C++ open-source code OpenFOAM 2.3.x using the *simpleFoam* solver for steady-state computations of incompressible flows. The Generalized Algebraic Multi-Grid solver was used for pressure, while all the other equations were solved with a *smoothSolver*. Convergence threshold was set to 10^{-7} for pressure and to 10^{-5} for the other quantities. Turbulence modelling relied on the low-Reynolds cubic model of [7] that allows for a partial reproduction of anisotropy of Reynolds stresses.

Grid details, computational domain and boundary conditions

The computational domain entails one blade-to-blade passage, with periodic boundary conditions imposed at mid-pitch. The domain extends 1 chord up- and 1.5 down-stream of the blade leading and trailing edge. The final computational grid entails 10.5M hexahedra clustered along the hub, casing and the blade profile, Figure 5. The mesh has 400 cells on the blade surface and 240 cells in radial direction, 30 of which are in the tip clearance. Mesh quality indicators are summarized in Table 2. The low skewness of the mesh was achieved using periodic boundaries with Arbitrary Mesh Interface technology. The inflow mass flow was specified, with a level of turbulence equal to 5 %. At the outlet of the domain convective boundary conditions were specified. Over the shroud velocity was imposed equal to zero, while for the blade and the hub velocity was imposed coherently with the full speed of the fan. k and ε were set to zero over all the solid walls following a well-known redefinition of the ε equation.

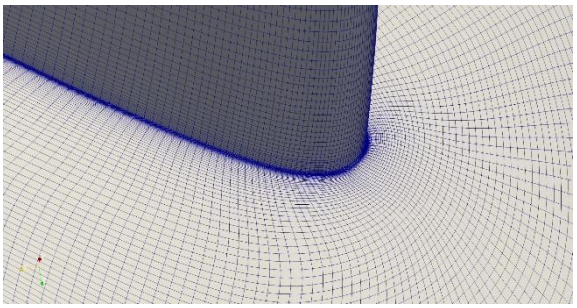

Figure 5 - Detail of the computational grid at the junction between blade and endwall

Table 2 - Mesh quality and y+ values

	Minimum	Maximum	Average
Volume ratio	1	4.8	1.1
Aspect ratio	1	160	9.7
Skewness	0	0.61	0.12
Min. included angle	23.5	90	63.5
y^+	0.67	5.2	2.77

Validation

Computations were performed using pressure rise and blade torque as convergence parameters. Results for this are summarized in Table 3 and confirm that the discrepancy of numerical data is within the margin of uncertainty of the experimental test-rig.

Table 3 - Datum blade CFD results vs experimental

	Measurements	*CFD*	*Δ*
$\Delta p\ [\psi]$	0.09323	0.09012	-3.3 %
η_{stat} [-]	56.0 %	57.8 %	1.8 %

CFD vs AxLab

In Figure 6 an analysis of the design quantities is carried out comparing spanwise distributions of velocity components and average flow angle computed by AxLab and OpenFOAM (CFD data were taken 1 chord downstream of the trailing edge of the blade).

As AxLab is an axis-symmetric solver, quantities derived from CFD computations were averaged on the circumferential direction. CFD results are provided also for the M-Fan, to address how the optimized geometry affected the flow field.

As a general comment, a good match between the 3D simulation results and the synthetic model numerical approach was found for most of the span of the blade. In fact the major differences are present near the hub and at the tip of the blade, where CFD computations can reproduce the physics of secondary motions and boundary layer development, that is neglected in AxLab.

In Figure 6 an axial velocity distribution shows that with respect to the M-Fan the L3C2 fan increases the flow rate in the lower 70 % of the blade and decreases the tip region resulting in unloading the tip. This is due to a strong reduction of the chord length in that region and it is reflected by a decrease in the same region of β_∞ and W_∞. A comparison of AxLab and CFD shows good agreement for the distribution of W_∞, while a discrepancy in axial velocity distribution is present, probably due to different inflow conditions (Axlab has a constant value of axial velocity while a distribution of velocity is applied in CFD computations).

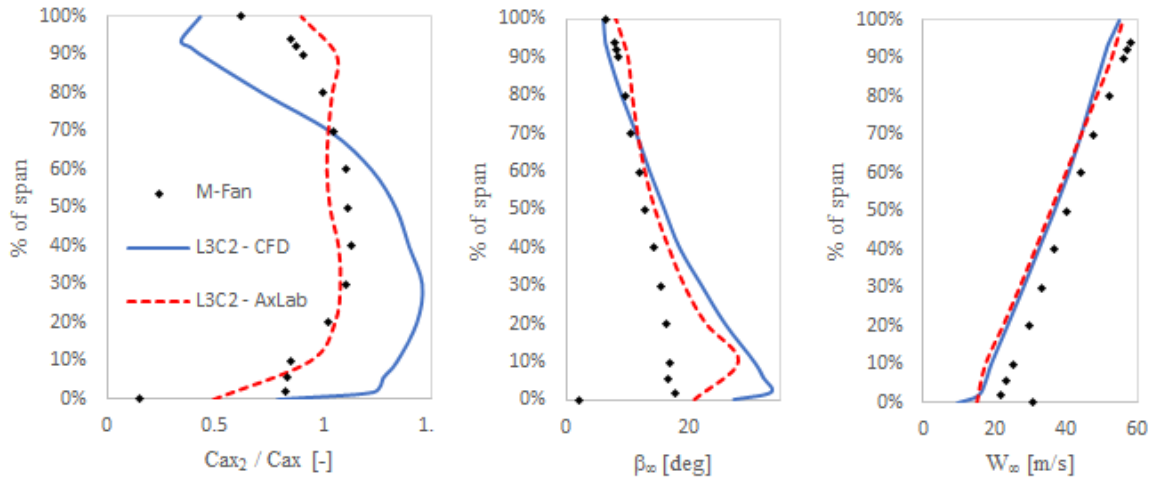

Figure 6 - Spanwise analysis of the optimized blade (AxLab & CFD) vs datum blade CFD

Mean flow survey

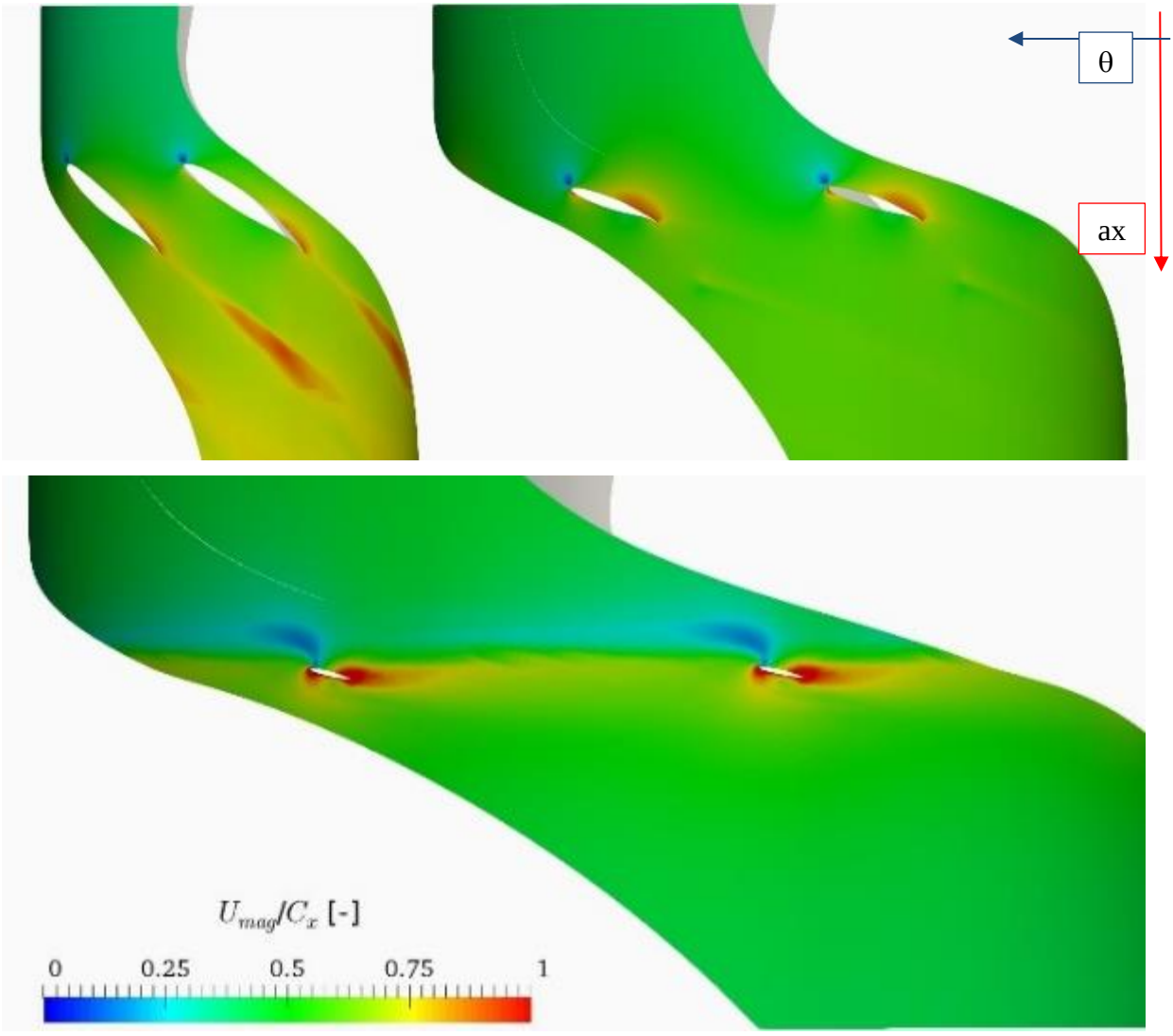

Figure 7 – Normalized velocity contours for different blade span (top-left) 10 %; (top-right) 50 %; (bottom) 98 %

From a series of velocity contours taken at different radial positions, it is possible to see that the flow is fully attached to the blade along all the blade span, Figure 7. The major visible structures are the wake of the blade, in particular near the hub of the rotor, and the tip leakage vortex.

These structures can be also visualized by means of helicity contours as shown in Figure 8, where an axial cross-section 0.5 chords downstream of the trailing edge is shown. At the hub of the blade the hub corner vortex is clearly recognizable. At the tip of the blade the tip leakage vortex develops along the casing and does not expand towards lower radii because of the blockage effect that results from the change in chord distribution at 70 % of the blade. The reduction of chord at higher radii results in a redistribution of flow that acts as a barrier and limits the possibility of the leakage vortex to expand towards lower radii.

Trailing edge noise.

The trailing edge noise was computed with the same model used for the optimization process, post-processing the flow field from CFD computations, resulting in a SPL reduction of -0.5 dB.

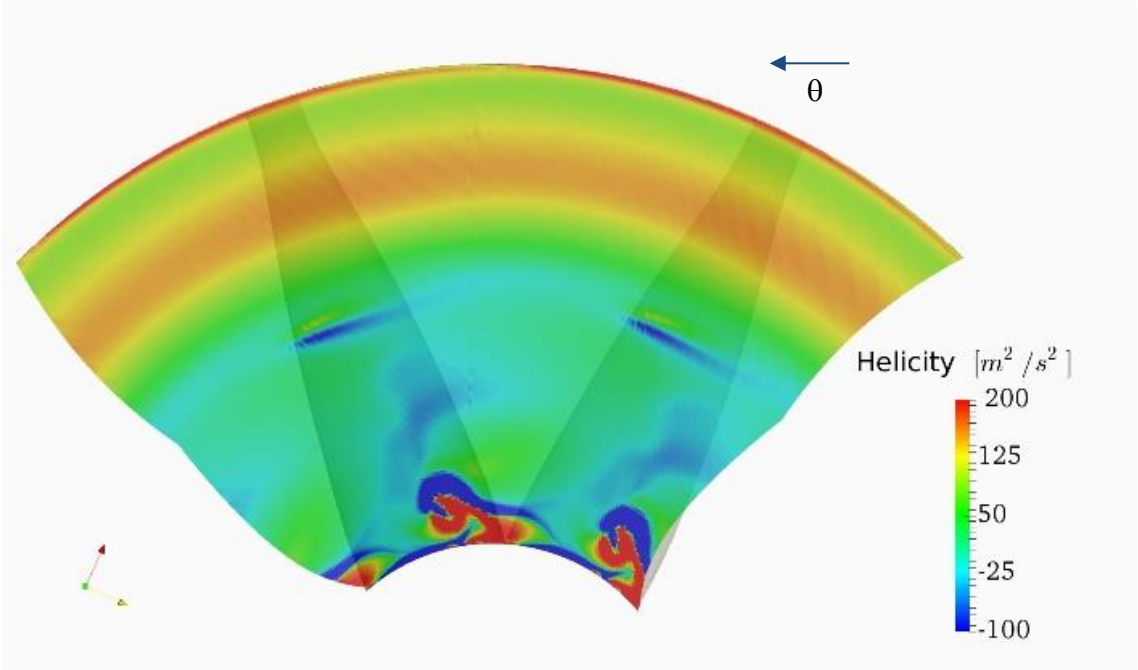

Figure 8 – Helicity field at 0.5c from the t.e. of the blade

CONCLUSIONS

We presented here the results of a brute-force optimization aiming at increasing the efficiency and decreasing the trailing edge noise of an axial flow fan for air-cooled condensers.

The algorithm generated a population of 200.000 individuals varying the pitch and chord distribution of a datum geometry and tested it using an axis-symmetric solver according to [5]. Among the 30 most promising individuals, one was chosen by comparison of blade load and diffusion factor distributions and comparing the different chord and pitch distributions.

The OPT blade was then tested with CFD to confirm the air performance in terms of static pressure rise and static efficiency, confirming that the individual is able to reach the design point of the fan.

Finally a prediction of trailing edge noise was carried out post-processing the velocity field and applying the same model, resulting in a reduction of -0.5 dB.

BIBLIOGRAPHY

[1] A. Corsini, F. Rispoli, A. G. Sheard - *Development of improved tip concept for low-noise operation in industrial fans*. IMechE J. of Power and Energy, 221, 669-681, **2007**.

[2] A. Corsini, F. Rispoli, A. G. Sheard - *Aerodynamic performance of blade-tip end-plates designed for low-noise operation in axial-flow fans*. Journal of Fluids Engineering, vol. 131, issue 8, 1-13, **2009**.

[3] S. Bianchi, A. Corsini, F. Rispoli, A. G. Sheard - *Detection of aerodynamic noise sources in low-speed axial fan with tip end-plates.* IMechE J. of Mechanical Engineering Science, Vol. 223, number 6, 1379-1392, **2009**.

[4] A. Corsini, G. Delibra, A. G. Sheard. - *The application of sinusoidal blade-leading edges in a fan-design methodology to improve stall resistance.* Proceedings of the Institution of Mechanical Engineers, Part A: Journal of Power and Energy May 2014 vol. 228 no. 3 255-271, 10.1177/0957650913514229, **2014**.

[5] T. Fukano, Y. Kodama, Y. Senoo - *Noise generated by low pressure axial flow fans, I: Modeling of the turbulent noise.* Journal of Sound and Vibration, Volume 50, Issue 1, 1977, Pages 63-74, ISSN 0022-460X, **1977**.

[6] L. Cardillo, A. Corsini, G. Delibra, A. G. Sheard, D. Volponi - *Axial Flow Fan Design Experience for a Project Based Turbomachinery Class*. ASME. Turbo Expo: Power for Land, Sea, and Air, Volume 6: Ceramics; Controls, Diagnostics and Instrumentation; Education; Manufacturing Materials and Metallurgy; Honors and Awards, **2015**

[7] Lien, F.S. & Leschziner, M.A. - *Assessment of Turbulence-transport Models Including Non-linear RNG Eddy-viscosity Formulation and Second-moment Closure for Flow over a Backward-facing Step*, Computers & Fluids vol. 23, pp. 983-1004, **1994**.